



# Obrabotka metallov - Metal Working and Material Science

Journal homepage: [http://journals.nstu.ru/obrabotka\\_metallov](http://journals.nstu.ru/obrabotka_metallov)



## The concept of microsimulation of processes of joining dissimilar materials by plastic deformation

Denis Salikhyanov<sup>1, 2, a, \*</sup>, Nikolay Michurov<sup>2, 3, b</sup>

<sup>1</sup> Institute of New Materials and Technologies, Ural Federal University named after the first President of Russia B.N. Yeltsin, 19 Mira Str., Ekaterinburg, 620002, Russian Federation

<sup>2</sup> Institute of Engineering Science, Ural Branch of the Russian Academy of Sciences, 34 Komsomolskaya Str., Ekaterinburg, 620049, Russian Federation

<sup>3</sup> Ural Institute of State Fire Service of EMERCOM of Russia, 22 Mira Str., Ekaterinburg, 620062, Russian Federation

<sup>a</sup>  <https://orcid.org/0000-0001-7235-7111>,  [d.r.salikhianov@urfu.ru](mailto:d.r.salikhianov@urfu.ru), <sup>b</sup>  <https://orcid.org/0000-0003-1775-6181>,  [n.michurov@ya.ru](mailto:n.michurov@ya.ru)

### ARTICLE INFO

#### Article history:

Received: 16 June 2023

Revised: 28 June 2023

Accepted: 06 July 2023

Available online: 15 September 2023

#### Keywords:

Laminated composites

Aluminum alloys

Joint deformation

Stress-strain state

Materials bonding

Finite element simulation

#### Funding

This study was performed in the frame of the grant № 22-29-20243 “Multi-scale simulation of processes of joining dissimilar materials by plastic deformation” funded by the Russian Science Foundation with the support of the government of Sverdlovsk region.

#### Acknowledgements

Research was partially conducted at core facility “Structure, mechanical and physical properties of materials”.

### ABSTRACT

**Introduction.** Bond strength between dissimilar materials is the most important characteristic of laminated composites, which determines the success of its development for industrial use. In order to develop the theory of joining materials by plastic deformation, it is proposed to perform computer simulation of joint deformation of representative volumes of dissimilar materials on a microscale and compare the parameters of the stress-strain state with the previously presented theoretical mechanism. **The aim of this work** is to analyze the stress-strain state of dissimilar materials under plastic deformation on a microscale and to establish the location of the onset of fracture of surface oxide films. To achieve this aim, **the following tasks** of the work are formulated: 1) to study the surface profiles of dissimilar materials to be bonded by plastic deformation; 2) to simulate by the finite element method (*FE*) the plastic deformation of contact surfaces of dissimilar materials on a microscale; 3) to study the stages of joint deformation of dissimilar materials on a microscale and verify of the theoretical mechanism. **Research methodology.** The study of three-dimensional topography and roughness was carried out on a *Veeco Wyko NT1100* Optical Profiling System. *Deform-3D FE* simulation package was chosen as the main research tool. Aluminum alloys *AMg3* and *D16* were chosen as the materials under study. **Results and discussion.** In this work, computer *FE* simulating of the joint deformation of the surface layers of *AMg3* and *D16* alloys on a microscale was performed, an analysis of the surface profiles of materials after various types of processing was carried out, the parameters of the stress-strain state were studied and compared with the parameters of the theoretical mechanism. Based on the results of the comparison, the adequacy of the proposed theoretical mechanism was assessed, and the practical difficulties of theoretical simulation of the joint deformation of dissimilar materials on the microscale were noted. Microscale *FE* simulation made it possible to study the flow of plastic deformation in the near-surface layers of materials, as well as to identify areas of the most probable fracture of surface oxide films and, consequently, areas of primary bonding of dissimilar materials.

**For citation:** Salikhyanov D.R., Michurov N.S. The concept of microsimulation of processes of joining dissimilar materials by plastic deformation. *Obrabotka metallov (tehnologiya, oborudovanie, instrumenty) = Metal Working and Material Science*, 2023, vol. 25, no. 3, pp. 36–49. DOI: 10.17212/1994-6309-2023-25.3-36-49. (In Russian).

#### \* Corresponding author

Salikhyanov Denis R., Ph.D. (Engineering), Associate Professor  
 Ural Federal University  
 named after the first President of Russia B.N. Yeltsin,  
 28 Mira Str., Ekaterinburg,  
 620002, Russian Federation  
**Tel.:** +7 (343) 375-44-37, **e-mail:** [d.r.salikhianov@urfu.ru](mailto:d.r.salikhianov@urfu.ru)

## Introduction

### *Influence of Roughness of Contact Surfaces on Bonding of Materials under Plastic Deformation*

Bond strength between dissimilar materials is the most important characteristic of laminated composites, which determines the success of its development for industrial production [1]. Among the known technologies for the production of laminated metal composites (explosion welding, cold roll bonding, powder coating, etc.), the most promising technologies are based on cold roll bonding due to the high process efficiency, the possibility of automation, and the relative ease of quality control. Compared with widespread explosion welding, laminated composites formed by deformation have higher accuracy, quality and stability of properties and a lower level of harmful tensile residual stresses.

A limiting factor in the development of production of laminated composites by rolling and other methods based on pressure is the problem of obtaining strong bonding between its layers [2]. Due to the complexity of ongoing physical and chemical processes at the interlayer boundary during plastic deformation, the determination of pressing modes is a laborious task for each new composite to be developed. As a result, the development of new technologies inevitably involves extensive experimental work.

Currently, a large number of studies on the influence of various factors of cold roll bonding on the bond strength between materials have been conducted [3–8]. *Jamaati and Toroghinejad* [3] and *Li et al.* [4] presented fairly detailed review papers describing the influence of factors on the bond strength between similar and dissimilar metals during cold roll bonding. In particular, *Jamaati and Toroghinejad* [3] determined the effect of reductions, annealing before and after rolling, initial sheet thickness, rolling speed, rolling direction, friction coefficient, and the presence of hardening particles. *Li et al.* [4] considered the effect of such rolling conditions as reduction, deformation zone parameters, the presence of contaminants and the thickness of the oxide film on the surfaces to be bonded, method of surface preparation, friction conditions, and post-annealing.

Review [3, 4] and experimental [9–17] works show that the preparation technology of contact surfaces of materials is one of the most significant factors influencing the process of its joining. Surface treatment is necessary to remove particles of moisture, grease and contaminating, as well as to reduce the thickness of surface oxide films that prevent bonding of materials. It is important to note that the optimal parameters of contact surfaces for joining materials are still unknown from the published works: the arithmetic mean roughness  $R_a$ , the height of asperities  $H$ , the mean step of asperities along the vertices  $S$ , the wavelength of asperities  $W$ , etc. For example, in [9], the highest strength of the steel-aluminum joint was obtained for surfaces with a roughness  $R_a$  of 5.8  $\mu\text{m}$  among the possible options of  $R_a$ : 1.7, 1.8, 1.9, 3.6, 4.2 and 5.8. The worst result was observed for surfaces with a roughness  $R_a$  equal to 1.8.

In [10], the maximum bond strength between brass and *IF* steel was obtained for a roughness  $R_a$  of the contact surfaces of 4.2  $\mu\text{m}$  among six options of roughness of the contact surfaces: 0.5, 1.7, 2.2, 2.9, 3.6 and 4.2  $\mu\text{m}$ . The worst result was when the roughness of the contact surfaces was 0.5  $\mu\text{m}$ .

In the works presented above, it was concluded that the greater the roughness of the contact surfaces, the higher the achievable bond strength between materials. The following are works in which this conclusion is not confirmed.

In [11], the best quality of the bonding between pure aluminum and aluminum alloy *AA2024* was observed for contact surfaces with a roughness  $R_a$  of less than 0.58  $\mu\text{m}$  among the possible options of 0.58, 0.13 and 0.03  $\mu\text{m}$  obtained by microengineering of surfaces, as well as 0.05 and 0.25 mm obtained by macroengineering. The worst quality was observed for surfaces with a roughness  $R_a$  equal to 0.2 mm.

In [12], the highest bond strength between pure aluminum and *AA2024* alloy was achieved at a contact surface roughness  $R_a$  of 1  $\mu\text{m}$  among the options: polished surface,  $R_a = 1, 3$  and 5  $\mu\text{m}$ . The worst result is obtained for a polished surface.

In [13], the maximum bond strength between sheets of commercially pure copper was achieved when the roughness of contact surfaces  $R_z$  was 0.09  $\mu\text{m}$  among the options of  $R_z = 0.09, 1.5, 4.4$  and 14  $\mu\text{m}$ . It was also found out in the work that the greater the ratio of the height  $H$  to the asperity base width  $W$  of the

profiles of contact surfaces, the greater the bond strength. It should be noted separately that the results of measuring  $H/W$  ratio were presented only in this work.

In [14], the highest bond strength between sheets of stainless martensitic steel  $1Cr11Ni2W2MoV$  was obtained for a contact surface roughness  $R_a$  of  $0.43 \mu\text{m}$  among two options of  $0.43$  and  $0.95 \mu\text{m}$ .

As can be seen from the last two works, a decrease in the roughness of the contact surfaces promotes the bonding between materials for certain conditions of accumulative roll bonding.

### *The mechanism of contact interaction between dissimilar materials during plastic deformation*

To develop the theory of material joint by plastic deformation and create new fundamental models, in the previous work of the author [18], a developed theoretical model of accumulative roll bonding of dissimilar materials was presented. The model assumed the contact of two materials, one of which is harder in relation to the other. Up to a certain limit of effective stress at the contact between materials, a harder material can be considered as ideally rigid. The model was developed under plane strain conditions. The stress analysis was carried out by the slip line method with the appropriate assumptions. The model considered the surface profile of only the hard material since the soft material was actively deformed at the first stages and took the form of the hard material. This assumption is indirectly confirmed in [10], where it was concluded that the influence of the surface roughness of a hard material is greater than that of a soft one.

Schematically, the model of bonding is shown in fig. 1 in the form of successive stages of deformation of the subsurface layers of materials:

1 – embedding of asperities of a harder material into a soft material. The soft material is squeezed out from under the asperities of hard material and flows into the cavities of the surface profile of hard material. The deformation zones are not in contact with each other.

2 – filling cavities on the surface of hard material with the soft material. The deformation zones are in contact. Common deformation zone is formed in the center, which is filled from under the neighboring asperities.

3 – the critical stage of filling the cavities on the surface of hard material with the soft one, whose flow is hindered by the influence of neighboring asperities. The unfilled parts of the cavities are residual pores at the interlayer boundary.

4 – propagation of plastic deformation into the deep layers of soft metal due to the damming created at the contact with the hard material.

Further filling of the cavities at the surface of hard material, as well as its plastic deformation, is possible only after hardening of the main volume of the soft material. From the point of view of bond formation, the moment and place of fracture of surface oxide films are important. According to the results of the theoretical analysis performed in [18, 19], the areas of the most probable fracture of the surface oxide layers were identified as follows:

1) areas of soft metal under the asperities, characterized by high values of accumulated plastic deformation  $\Lambda$  and low values of the relative average normal stress  $\sigma/T$ , which means the prevailing proportion of compressive stresses.  $\Lambda$  is the degree of shear deformation,  $\sigma$  is the mean stress, and  $T$  is the intensity of shear stresses.

2) areas of soft metal in the center of the free surface, characterized by low values of accumulated plastic deformation  $\Lambda$  and high values of the stress state index  $\sigma/T$ , corresponding to an increased proportion of tensile stresses.

Values of the stress-strain state and the volume of unfilled cavities vary in a wide range depending on the profile of hard material surface, expressed as the ratio of the height to the asperity base width  $H/W$  [18].

Due to limitations of the theoretical model, it is not possible to establish the location of fracture of oxide films and the subsequent initiation of the formation of bond bridges between pure metals. In addition, it is not known to what extent the developed theoretical model reflects the actual contact interaction of surfaces of dissimilar materials during plastic deformation.

In this regard, the **aim** of this work is to analyze the stress-strain state of dissimilar materials under plastic deformation on a microscale and to establish the location of the onset of fracture of surface oxide

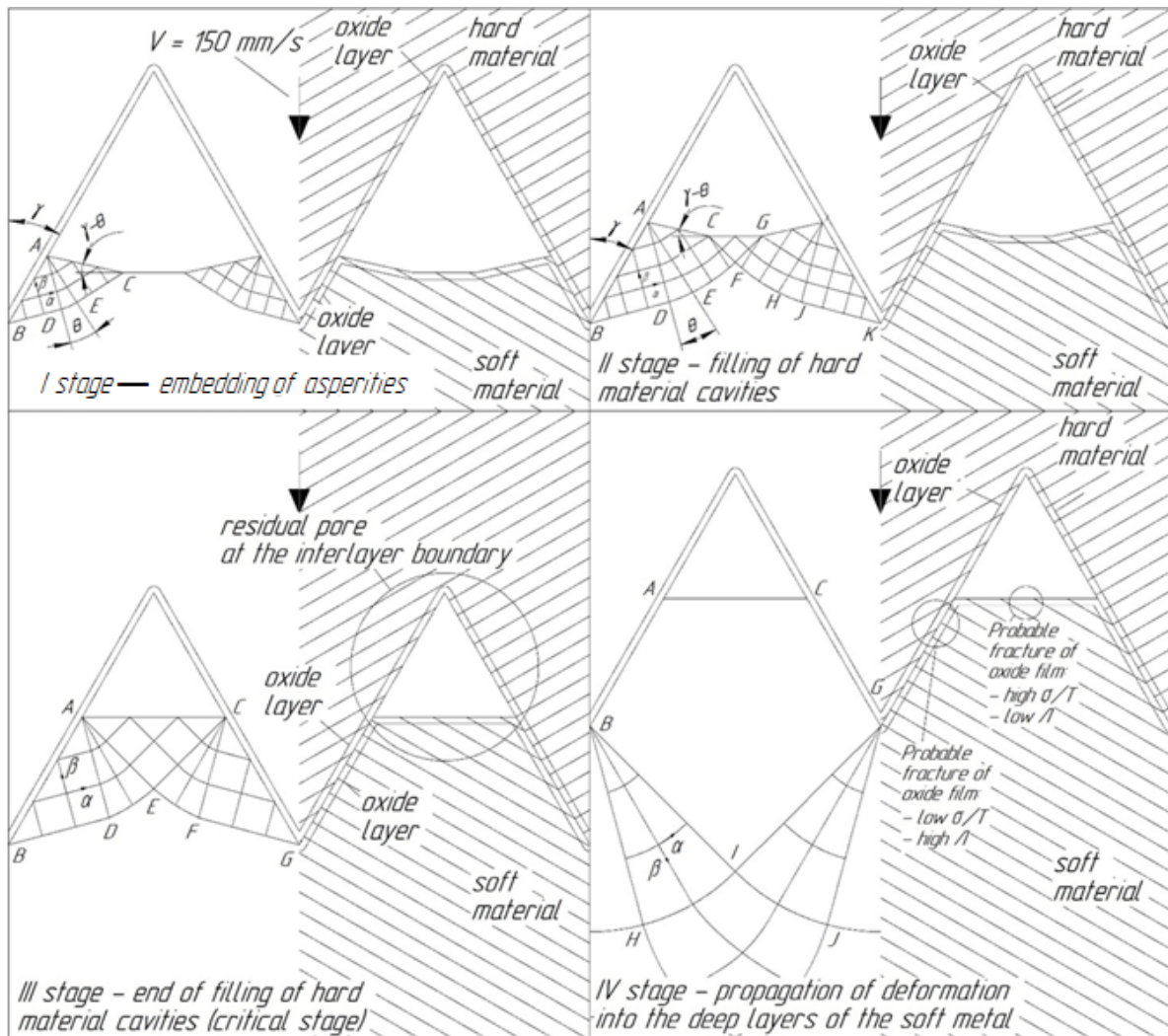


Fig. 1. Microscale theoretical model of plastic deformation of dissimilar materials

films. To achieve this aim, the following tasks of the work are formulated: 1) to study the surface profiles of dissimilar materials to be bonded by plastic deformation; 2) to simulate by the finite element method (FE) the plastic deformation of contact surfaces of dissimilar materials on a microscale; 3) to study the stages of joint deformation of dissimilar materials on a microscale and verify of the theoretical mechanism.

## Materials and methods

The object of study was the process of accumulative roll bonding of aluminum alloys *DI6* (alloy of the 2xxx series, strain- and age-hardenable) and *AMg3* (alloy of the 5xxx series, strain-hardenable) [20].

The surfaces of aluminum alloys to be bonded were degreased with acetone, dried, and machined before plastic deformation. Machining of the surfaces of the rolling billets was carried out according to two different modes: (a) belt grinding with 40 grit (medium grit) and (b) belt grinding with 120 grit (fine grit). Grinding was performed at a belt speed of 250 m/min with the grinding direction coinciding with the rolling direction.

The study of three-dimensional topography and roughness was carried out on a *Veeco Wyko NT1100* Optical Profiling System. As a result of the study, an array of coordinate points of the surface with an area of  $1159 \times 756 \mu\text{m}$  and roughness parameters were obtained: average roughness  $R_a$ , root mean square roughness  $R_q$ , and total height of the roughness profile  $R_t$ . The array of coordinate points was used to create a three-dimensional surface and three-dimensional representative volume elements of near-surface layers of materials with dimensions of  $1,159 \times 756 \times 600$  ( $L \times W \times H$ ) for microscale FE simulation.

Sheets from *DI6* and *AMg3* alloys were supplied in the annealed (soft) state. The hardening curves of these alloys were obtained using a cam plastometer of *IES Ural Branch of the Russian Academy of Sciences* and then integrated into the *Deform 3D* environment. The resulting strain resistance ratio  $\frac{\sigma_{DI6}}{\sigma_{AMg3}}$

of the alloys was close to 0.8.

The *Deform-3D FE* simulation package was chosen as the main research tool. To save computational resources during solving problems, density windows with a size of *FE* inside the windows of 22–23  $\mu\text{m}$  and outside the windows of 50  $\mu\text{m}$  were used. Before plastic deformation, representative volume elements were brought into contact, as shown in fig. 2, with specified boundary conditions. In order to prevent displacement of one representative volume relative to another, as well as to prevent loss of stability, the boundary condition  $v_y = 0 \mu\text{m/s}$  was set on one of the faces. On the upper face of the representative volume element of *AMg3* alloy, which is opposite to the surface of the asperities, the displacement velocity  $v_z = 150 \mu\text{m/s}$  was applied. Under the influence of the created force, plastic deformation occurred in both materials at a certain moment. The process of plastic deformation continued until the maximum value of strain resistance of *DI6* alloy was reached.

## Results and discussion

### Study of surface profiles

At the first stage of the study, solid models of representative volumes of *AMg3* and *DI6* alloys after 40 and 120 grit belt grinding were obtained. An example of a model for the *AMg3* alloy processed by a 40 grit belt is shown in fig. 3. Due to the chosen type of surface machining, a longitudinal profile was obtained

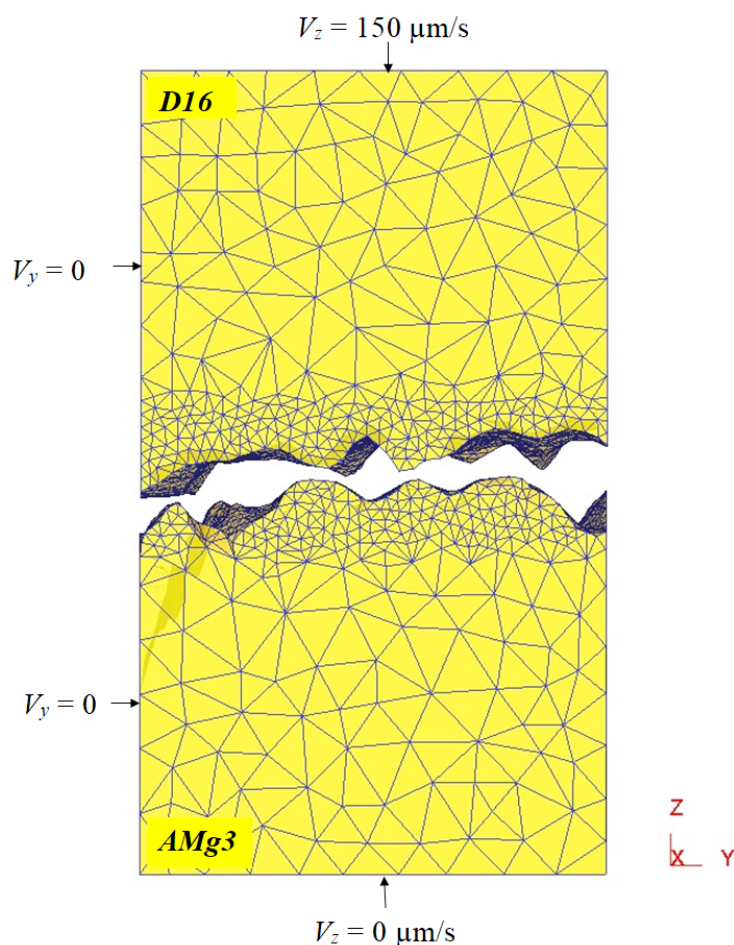


Fig. 2. Problem statement of microscale simulation of the process of plastic deformation of alloys *AMg3* and *DI6*

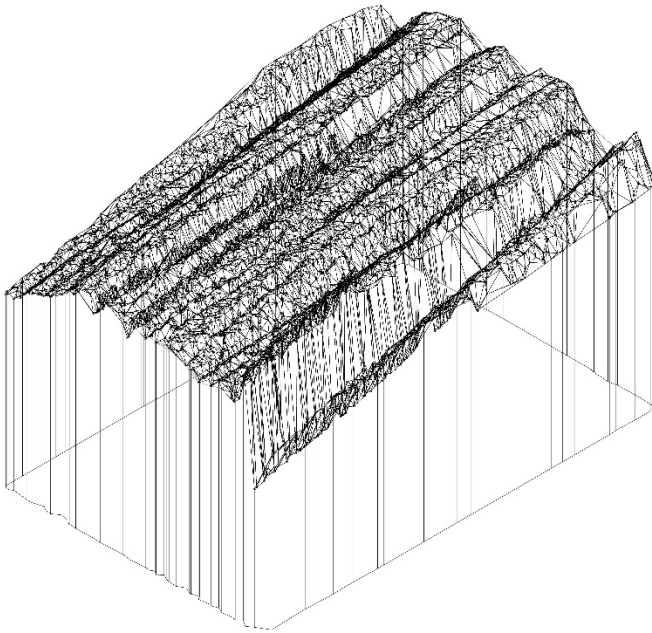


Fig. 3. Representative volume of *AMg3* alloy with surface machined by a grinder with a 40 grit band

for all materials, as shown in fig. 3. Therefore, the simulated processes can be considered in the context of comparison with a theoretical model in a flat setting.

The created solid models were analyzed in separate sections through a step of 100  $\mu\text{m}$  to establish the average values of the actual ratio of height to asperity base width  $H/W$  or the actual value  $\frac{1}{2} \text{ctg}(\alpha)$ , where  $\alpha$  is the asperity top angle. An example of the analysis of cross sections of representative volumes of materials after different types of surface machining is shown in fig. 4. As can be seen in fig. 4, the surface profile of materials after machining is a set of randomly arranged figures of various shapes and sizes. Based on visual observation, the most suitable geometric figures for describing the section of surface profiles are triangles and trapezoids.

The results of estimating the surface profile parameters  $\alpha$  and  $H/W$  are summarized in Table 1. It can be seen that the same type of surface machining creates different surface profiles depending on the material, which is primarily due to the strength characteristics and hardness of the materials being machined. The softer the material (annealed *D16* in our case),

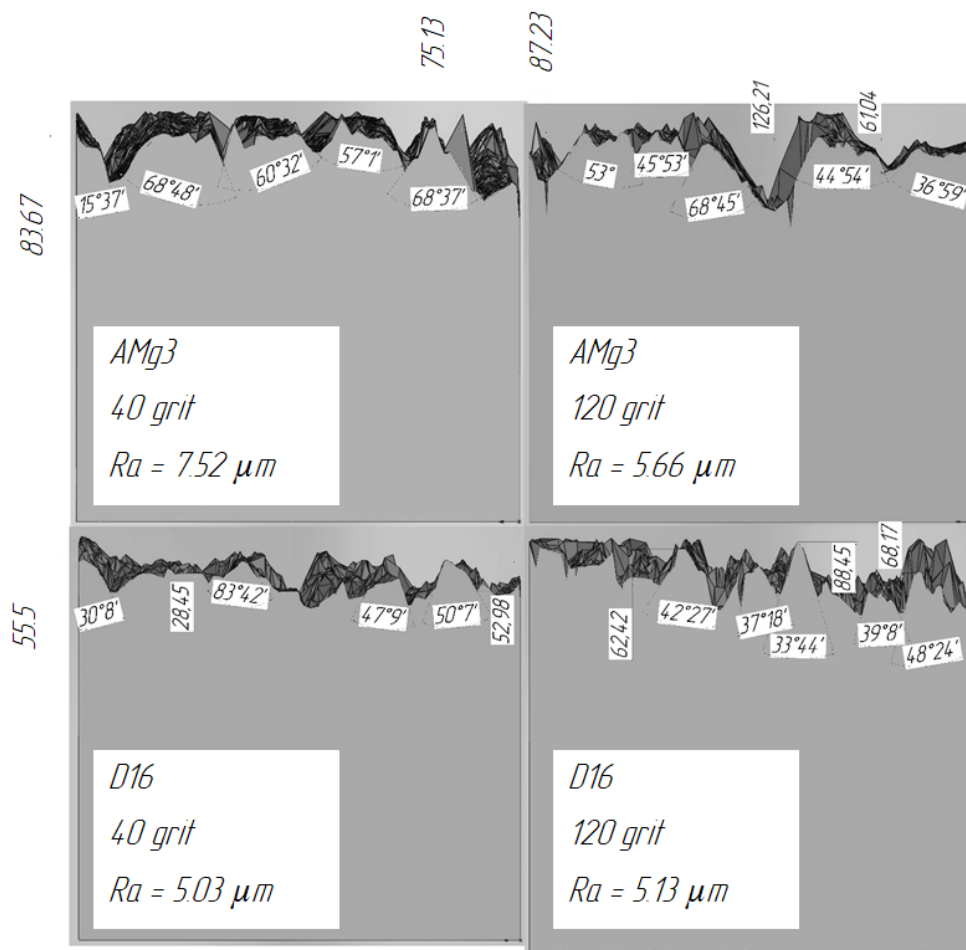


Fig. 4. Cross-sections of representative volumes of *AMg3* and *D16* alloys after grinding with 40 and 120 grit bands

**Surface topography parameters of AMg3 and D16 alloys after grinding with 40 and 120 grit bands**

Material/type of grinding	Average roughness $R_a$ , $\mu\text{m}$	Total height of profile $R_t$ , $\mu\text{m}$	Average angle of the top of asperities	The ratio of the height of asperity to the width of asperity base
AMg3/40 grits	7.52	126.19	57°	0.33
AMg3/120 grits	5.66	116.19	49°	0.43
D16/40 grits	5.03	46.24	60°	0.29
D16/120 grits	5.13	55.15	40°	0.6

the lower the roughness parameters  $R_a$  and  $R_t$  are. Grinding by belts with different grits had an unequal effect on the materials under study. Changing the grain size of belts from 40 to 120 grits led to a decrease in the roughness parameters  $R_a$  and  $R_t$  and to a decrease in the average asperity top angle of the AMg3 alloy. At the same time, there was a slight increase in the roughness parameters  $R_a$  and  $R_t$  and a decrease in the average asperity top angle of the D16 alloy. The obtained average asperity top angles for all materials are in the range of 40–60°, and the ratio of the asperity height to the asperity base width  $H/W$  is in the range of 0.29–0.6.

According to the theoretical model [18], the relative penetration depth  $h/H$  should lie in the range of 0.56–0.64 by the time the plastic deformation begins to propagate in the bulk of the soft material, where  $h_t$  is the depth of penetration of hard material asperities into the soft material. The reduced normal stress  $\sigma/k$  at the contact of materials should be in the range from  $-2.4$  to  $-3.09$ , where  $k$  is the shear strain resistance of the soft material.

#### *Study of Plastic Deformation of Dissimilar Materials on a Microscale*

As indicated in the research methodology, the surface profiles of AMg3 and D16 materials were brought into contact, after which plastic deformation was initiated. Fig. 5 shows the initial moment of contact of the materials' surfaces after belt grinding with 40 and 120 grits in a random central section of representative volumes. As can be seen, the actual pattern of contact between materials in this section does not repeat the idealized theoretical model in its pure form: periodically repeating asperities have different shapes and sizes; opposite the asperities of one material, both asperities and cavities of another material can be located. Accordingly, the stages described in 1.2, will occur non-simultaneously over the entire contact area during the process of plastic deformation.

To assess the stages of accumulative roll bonding of dissimilar materials, the effective strain intensity scale was adjusted with an upper threshold level of 120 MPa, which is equivalent to the yield strength of AMg3 alloy. When the nodal points of FE reached 120 MPa, the corresponding areas of the materials were highlighted in red, which meant the transition of the material to the plastic state. When the entire volume of both materials reached 120 MPa, the scale was reconfigured to the next upper level of 200 MPa, which corresponded to the maximum value of the strain resistance of the D16 alloy. The key stages of accumulative roll bonding of materials preliminary grinded by 40 grit belt are shown in fig. 6, and those preliminary grinded by 120 grit belt are shown in fig. 7.

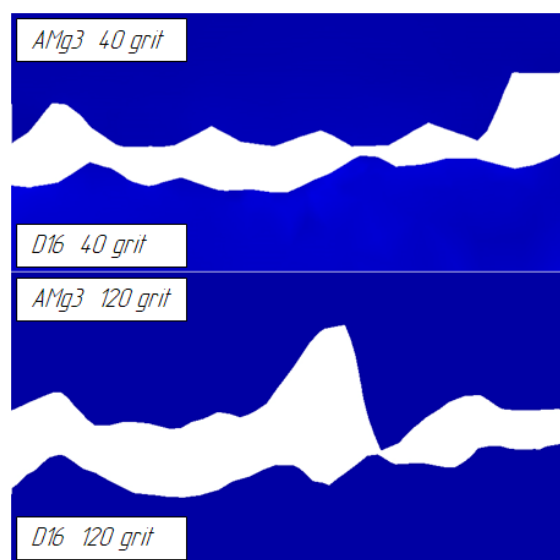


Fig. 5. Contact of surfaces of AMg3 and D16 alloys before plastic deformation in a random cross-section

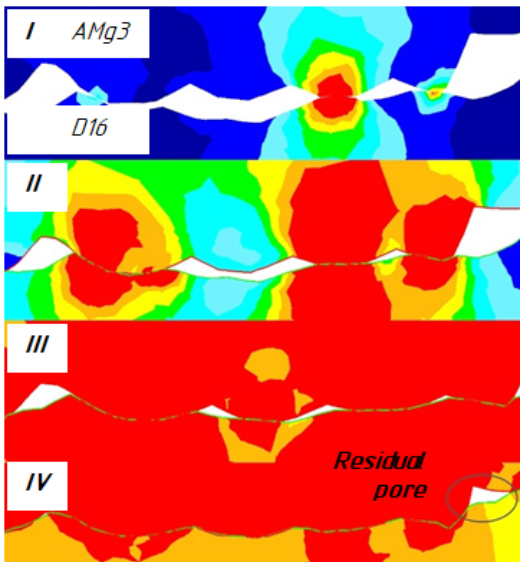


Fig. 6. Stages of joint plastic deformation of *AMg3* and *D16* alloys preliminary grinded with a 40 grit band

stages proceed in accordance with the proposed theoretical mechanism.

At **stage III** of the accumulative roll bonding micromodel, the relative penetration depth  $h/H$  and the reduced normal stress at the contact of materials  $\sigma/k$  were evaluated and compared with the theoretical model [18] (Table 2). As can be seen from Table 2, the relative penetration depth of asperities  $h/H$  of the *FE* micromodel differs significantly from the results of calculation by the theoretical model. The discrepancy is primarily due to significant differences between the actual profiles of material surfaces from the theoretical ones, as well as the closeness of strain resistances of materials, which resulted in almost simultaneous materials' deformation.

The discrepancies in the reduced normal stresses  $\sigma/k$ , obtained through the *FE* micromodel and the theoretical model, are also noticeable, which is explained by the closeness of the strain resistances of the material and its almost simultaneous transition to the plastic state. As a result, the theoretical model [18] gives only approximate values of the stress-strain state indicators for the processes under consideration.

An important practical aspect of *FE* microsimulation was the determination of areas of the most probable fracture of surface oxide layers. As a criterion for assessing the probability of fracture, the well-known *Cockcroft-Latham* criterion was used

$$\int_0^{\bar{\epsilon}^p} \frac{\sigma_1}{\bar{\sigma}} d\bar{\epsilon},$$

where  $\sigma_1$  is the principal stress,  $\bar{\sigma}$  is the effective

stress, and  $d\bar{\epsilon}$  is the accumulated plastic strain increment. Fig. 8 shows the contact surface on the side of *D16* alloy at the beginning of **stage III** of accumulative roll bonding with highlighted contact points with *AMg3* surface and without contact points. Fig. 8 demonstrates that the highest values of damage of the surface layers are observed in areas free from contact with the opposite material.

As shown in figs. 6 and 7, the flow of materials at the **stage I** of bond deformation is quite different from the idealized representation: plastic deformation of both *D16* alloy and harder *AMg3* alloy begins almost simultaneously. An analysis of the deformation of representative volumes shows that the asperities of both materials crumble simultaneously. This is primarily due to the closeness of the strain resistances of the alloys, whose ratio is close to 0.8. By the end of critical **stage II**, unfilled sections of cavities remain at the interface between materials due to insufficient applied pressures, while plastic deformation begins to propagate deep into the bulk of both materials (**stage III**).

As the work hardening of both materials increases and the pressure at the interlayer boundary increases, the cavities on *AMg3* alloy surface are filled up. When the maximum value of the effective stress of the *D16* alloy is reached, unfilled cavities remain at the interlayer boundary (residual pores). A further increase in pressure is required to fill it. Thus, despite the differences at the first stage of joint plastic deformation, the final

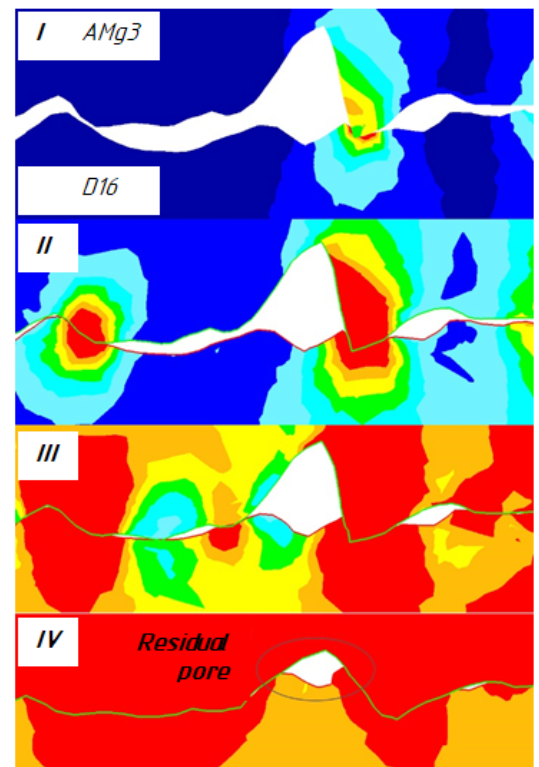


Fig. 7. Stages of joint plastic deformation of *AMg3* and *D16* alloys preliminary grinded with a 120 grit band

The results of comparing the parameters of the stress-strain state of the *FE* micromodel with the theoretical mechanism [18]

Materials/type of grinding	Relative penetration depth $h/H$		Reduced normal stress $\sigma/k$	
	Theoretical model [18]	<i>FE</i> micro model	Theoretical model [18]	<i>FE</i> micro model
<i>AMg3-D16/40</i> grit	0.62	0.86	-2.92	-2.45
<i>AMg3-D16/120</i> grit	0.61	0.4	-2.75	-1.9

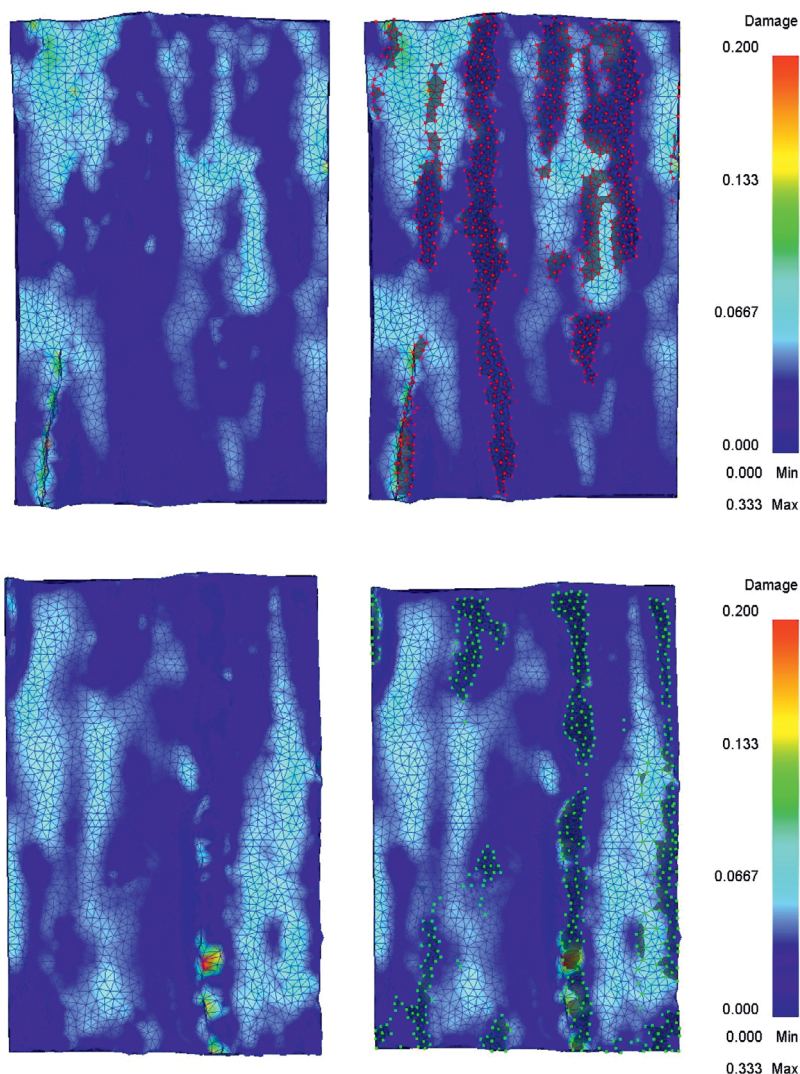


Fig. 8. Areas of the most probable fracture of the surface oxide layers on the *D16* alloy

Hence, it follows that a more significant factor in the fracture of surface oxide films is the high values of the stress state index  $\sigma/T$ , which are characteristic of surfaces free from contact with the opposite material.

## Conclusion

In this work, computer *FE* simulation of macroscale processes of accumulative roll bonding occurring on the surfaces of *AMg3* and *D16* alloys is performed. An analysis of the surface profiles of materials after various modes of grinding is carried out. The parameters of stress-strain state were studied and compared with the same parameters of the theoretical mechanism.

Comparison of the parameters showed noticeable discrepancies at the **stage I** and **stage II** of joint deformation, which is associated with close values of strain resistances of the materials to be bonded and the deviation of the actual surface profiles from the idealized ones. Despite this, after the onset of the critical **stage III**, further joint deformation proceeds in accordance with the proposed theoretical mechanism: unfilled sections of cavities remain at the interface between the materials, and plastic deformation begins to propagate deep into the bulk of both materials. As the work hardening of both materials increases and the pressure at the interlayer boundary increases, the cavities on the alloy surface are filled up.

Thus, *FE* modeling of joint deformation on a microscale made it possible to identify the limits of application of the theoretical mechanism, discrepancies in the case of joint deformation of materials with similar values of strain resistance, and directions for further improvement. The theoretical model is recommended to be used to analyze the processes of joint deformation of materials with a greater difference in strain resistance. When studying the processes of deformation of materials with similar values of strain resistance, the model adequately reflects the sequence after the onset of the critical stage, namely, at the moment of the onset of propagation of plastic deformation deep into the bulk of materials. To expand the boundaries of using the theoretical model, it is recommended to consider the problem of plastic crumpling of the asperities.

### References

1. Groche P., Wohletz S., Brenneis M., Pabst C., Resch F. Joining by forming – A review on joint mechanisms, applications and future trends. *Journal of Materials Processing Technology*, 2014, vol. 214, pp. 1972–1994. DOI: 10.1016/j.jmatprotec.2013.12.022.
2. Mori K.-I., Bay N., Fratini L., Micari F., Tekkaya A.E. Joining by plastic deformation. *CIRP Annals – Manufacturing Technology*, 2013, vol. 62, pp. 673–694. DOI: 10.1016/j.cirp.2013.05.004.
3. Jamaati R., Toroghinejad M.R. Cold roll bonding bond strengths: review. *Materials Science and Technology*, 2011, vol. 27, iss. 7, pp. 1101–1108. DOI: 10.1179/026708310X12815992418256.
4. Li L., Nagai K., Yin F. Progress in cold roll bonding of metals. *Science and Technology of Advanced Materials*, 2008, vol. 9, p. 023001. DOI: 10.1088/1468-6996/9/2/023001.
5. Rezayat M., Akbarzadeh A. Bonding behavior of Al–Al<sub>2</sub>O<sub>3</sub> laminations during roll bonding process. *Materials and Design*, 2012, vol. 36, pp. 874–879. DOI: 10.1016/j.matdes.2011.08.048.
6. Tang C., Liu Z., Zhou D. Surface treatment with the cold roll bonding process for an aluminum alloy and mild steel. *Strength of Materials*, 2015, vol. 47, iss. 1, pp. 150–155. DOI: 10.1007/s11223-015-9641-3.
7. Arbo S.M., Westermann I., Holmedal B. Influence of stacking sequence and intermediate layer thickness in AA6082-IF steel tri-layered cold roll bonded composite sheets. *Key Engineering Materials*, 2018, vol. 767, pp. 316–322. DOI: 10.4028/www.scientific.net/KEM.767.316.
8. Gao C., Li L., Chen X., Zhou D., Tang C. The effect of surface preparation on the bond strength of Al–St strips in CRB process. *Materials and Design*, 2016, vol. 107, pp. 205–211. DOI: 10.1016/j.matdes.2016.05.112.
9. Akdesir M., Zhou D., Foadian F., Palkowski H. Study of different surface pre-treatment methods on bonding strength of multilayer aluminum alloys/steel clad material. *International Journal of Engineering Research & Science*, 2016, vol. 2, iss. 1, pp. 169–177.
10. Bagheri A., Toroghinejad M.R., Taherizadeh A. Effect of roughness and surface hardening on the mechanical properties of three-layered brass/IF steel/brass composite. *Transactions of the Indian Institute of Metals*, 2018, vol. 71, iss. 9, pp. 2199–2210. DOI: 10.1007/s12666-018-1351-7.
11. Liu J., Li M., Sheu S., Karabin M.E., Schultz R.W. Macro- and micro-surface engineering to improve hot roll bonding of aluminum plate and sheet. *Materials Science and Engineering A*, 2008, vol. 479, pp. 45–57. DOI: 10.1016/j.msea.2007.06.022.
12. Mikloweit A., Bambach M., Pietryga M., Hirt G. Development of a testing procedure to determine the bond strength in joining-by-forming processes. *Advanced Materials Research*, 2014, vol. 966–967, pp. 481–488. DOI: 10.4028/www.scientific.net/AMR.966-967.481.
13. Wang A., Ohashi O., Ueno K. Effect of surface asperity on diffusion bonding. *Materials Transactions*, 2006, vol. 47, iss. 1, pp. 179–184. DOI: 10.2320/matertrans.47.179.
14. Zhang Ch., Li H., Li M. Role of surface finish on interface grain boundary migration in vacuum diffusion bonding. *Vacuum*, 2017, vol. 137, pp. 49–55. DOI: 10.1016/j.vacuum.2016.12.021.



15. Wang Ch., Jiang Y., Xie J., Zhou D., Zhang X. Effect of the steel sheet surface hardening state on interfacial bonding strength of embedded aluminum–steel composite sheet produced by cold roll bonding process. *Materials Science & Engineering A*, 2016, vol. 652, pp. 51–58. DOI: 10.1016/j.msea.2015.11.039.
16. Danesh Manesh H., Shahabi H.Sh. Effective parameters on bonding strength of roll bonded Al/St/Al multilayer strips. *Journal of Alloys and Compounds*, 2009, vol. 476, iss. 1–2, pp. 292–299. DOI: 10.1016/j.jallcom.2008.08.081.
17. Jamaati R., Toroghinejad M.R. The role of surface preparation parameters on cold roll bonding of aluminum strips. *Journal of Materials Engineering and Performance*, 2011, vol. 20, iss. 2, pp. 191–197. DOI: 10.1007/s11665-010-9664-7.
18. Salikhyanov D. Contact mechanism between dissimilar materials under plastic deformation. *Comptes Rendus Mecanique*, 2019, vol. 347, pp. 588–600. DOI: 10.1016/j.crme.2019.07.002.
19. Bogatov A., Salikhyanov D. Development of bonding mechanisms for different materials during forming. *Metallurgist*, 2017, vol. 60, iss. 11–12, pp. 1175–1179. DOI: 10.1007/s11015-017-0424-x.
20. Burkin S.P., Babailov N.A., Ovsyannikov B.V. *Soprotivlenie deformatsii splavov Al i Mg* [Deformation resistance of Al and Mg alloys]. Ekaterinburg, UrFU Publ., 2010. 344 p. ISBN 978-5-321-01755-5.

## Conflicts of Interest

The authors declare no conflict of interest.

© 2023 The Authors. Published by Novosibirsk State Technical University. This is an open access article under the CC BY license (<http://creativecommons.org/licenses/by/4.0>).

